

Capsaicin-induced apoptosis of glioma cells is mediated by TRPV1 vanilloid receptor and requires p38 MAPK activation

C. Amantini,* M. Mosca,†* M. Nabissi,* R. Lucciarini,* S. Caprodossi,†* A. Arcella,‡
F. Giangaspero†‡ and G. Santoni*

*Department of Experimental Medicine and Public Health, University of Camerino, Camerino, Italy

†Department of Experimental Medicine, University of Rome, "La Sapienza", Rome, Italy

‡Istituto Neurologico Mediterraneo Neuromed, Pozzilli, Italy

Abstract

We provide evidence on the expression of the transient receptor potential vanilloid type-1 (TRPV1) by glioma cells, and its involvement in capsaicin (CPS)-induced apoptosis. TRPV1 mRNA was identified by quantitative RT-PCR in U373, U87, FC1 and FLS glioma cells, with U373 cells showing higher, and U87, FC1 and FLS cells lower TRPV1 expression as compared with normal human astrocytes. By flow cytometry we found that a substantial portion of both normal human astrocytes, and U87 and U373 glioma cells express TRPV1 protein. Moreover, we analyzed the expression of TRPV1 at mRNA and protein levels of glioma tissues with different grades. We found that TRPV1 gene and protein expression inversely correlated with glioma grading, with marked loss of TRPV1 expression in the majority of grade IV glioblastoma

multiforme. We also described that CPS trigger apoptosis of U373, but not U87 cells. CPS-induced apoptosis involved Ca^{2+} influx, p38 but not extracellular signal-regulated mitogen-activated protein kinase activation, phosphatidylserine exposure, mitochondrial permeability transmembrane pore opening and mitochondrial transmembrane potential dissipation, caspase 3 activation and oligonucleosomal DNA fragmentation. TRPV1 was functionally implicated in these events as they were markedly inhibited by the TRPV1 antagonist, capsazepine. Finally, p38 but not extracellular signal-regulated protein kinase activation was required for TRPV1-mediated CPS-induced apoptosis of glioma cells.

Keywords: apoptosis, brain tumors, capsaicin, cell death, glioma, transient receptor potential vanilloid-1.

J. Neurochem. (2007) **102**, 977–990.

Malignant gliomas are the most common type of primary brain tumors (Maher *et al.* 2001). Diffuse gliomas are classified histologically according to the hypothesized line of glial differentiation as astrocytomas, oligodendrogliomas or tumors with morphological features of both astrocytes and oligodendrocytes, called oligoastrocytomas. Astrocytomas are pathologically graded in accordance with the World Health Organization as low grade (grade II), anaplastic astrocytoma (grade III) or high grade (grade IV), glioblastoma multiforme. Oligodendrogliomas and oligoastrocytomas are graded as low grade (grade II) or anaplastic (grade III). Glioblastoma multiforme is the most aggressive and prevalent type of glioma, accounting for at least 80% of malignant gliomas (Maher *et al.* 2001; Kleihues *et al.* 2002). Despite recent advances in therapy, significant progress in accurate prognosis and improved survival have not been achieved so far (Maher *et al.* 2001).

Received October 17, 2006; revised manuscript received January 19, 2007; accepted March 1, 2007.

Address correspondence and reprint requests to Prof. Giorgio Santoni, Department of Experimental Medicine and Public Health, University of Camerino, Via Scalzino 3, 62032 Camerino, Italy.

E-mail: giorgio.santoni@unicam.it

Abbreviations used: $[Ca^{2+}]_i$, intracellular free calcium; AEA, anandamide; CPS, capsaicin; CPZ, capsazepine; CSA, cyclosporine A; EB, epileptic brain; ERK, extracellular signal-regulated protein kinase; FCS, fetal calf serum; FITC, fluorescein isothiocyanate; HRP, horseradish peroxidase; JC-1, 5,5',6,6'-tetrachloro-1,1',3,3'-tetraethylbenzimidazolylcarbocyanine iodide; mAb, monoclonal antibody; MAPK, mitogen-activated protein kinase; MFI, mean fluorescence intensity; MTT, 3-(4,5-dimethylthiazol-2-yl)-2,5-diphenyltetrazolium bromide; NHA, normal human astrocytes; NHNPC, normal human neural progenitor cells; PBMC, peripheral blood mononuclear cells; PBS, phosphate-buffered saline; PI, propidium iodide; PS, phosphatidylserine; PTP, permeability transmembrane pore; RAG, rabbit anti-goat; SDS-PAGE, sodium dodecyl sulfate-polyacrylamide gel electrophoresis; TRPV1, transient receptor potential vanilloid type-1; $\Delta\Psi_m$, mitochondrial transmembrane potential.

Apoptosis pathway is often disrupted in tumor cells (Thompson 1995) and particularly in malignant gliomas (Grossman and Batarra 2004). Therefore, restoration of the apoptotic pathway or introduction of pro-apoptotic molecules may represent a very attractive strategy for the treatment of these tumors.

The neurotoxin capsaicin (CPS), has been utilized as a specific tool for sensory afferent neurons, and is widely used in neurophysiological and immunopharmacological studies (Holzer 1991; Santoni *et al.* 1999, 2000, 2004). Many of the acute cellular and physiologic effects associated with CPS exposure are mediated by the transient receptor potential vanilloid type-1 (TRPV1), a non-selective cation channel structurally related to members of the transient receptor potential family of ion channels (Szallasi and Blumberg 1999). TRPV1 is mainly expressed by primary sensory neurons involved in nociception and neurogenic inflammation (Holzer 1991; Caterina *et al.* 1997; Caterina and Julius 2001).

In addition to CPS TRPV1 is activated by heat (Caterina *et al.* 1997, 2000) as well as by chemical mediators, including acid pH and lipid mediators, including anandamide (AEA) and eicosanoids (Szallasi and Blumberg 1999; Gunthorpe *et al.* 2002).

Several studies have shown the capacity of CPS to inhibit *in vivo* and *in vitro* the growth of tumor cells such as adenocarcinoma, leukemia and glioblastoma cells (Lee *et al.* 2000; Hail 2003; Kang *et al.* 2003; Ito *et al.* 2004; Qiao *et al.* 2005; Mori *et al.* 2006) by inducing apoptosis, but the mechanism/s underlying CPS-mediated pro-apoptotic effects have been not completely elucidated yet.

Capsaicin-induced cell death involves TRPV1 in response to low doses of neurotoxin in a variety of normal and neoplastic cell types (Caterina *et al.* 1997; Biro *et al.* 1998; Grant *et al.* 2002; Amantini *et al.* 2004), whereas high doses and/or long-term exposure to CPS result in TRPV1-independent cell death (Hail 2003).

Aim of the present study was to investigate the expression of TRPV1 in glioma tissues of different grading and in a number of primary and established cell lines, as well as its involvement in CPS-induced glioma cell apoptosis. Moreover, we examined some of the molecular mechanisms underlying CPS-induced TRPV1-mediated apoptosis, namely intracellular free calcium ($[Ca^{2+}]_i$) influx, mitogen-activated protein kinase (MAPK) activation, mitochondrial transmembrane potential ($\Delta\Psi_m$) dissipation, caspase 3 activation and oligonucleosomal DNA fragmentation.

Materials and methods

Cells and tissues

Epileptic brain (EB), astrocytoma, oligoastrocytoma, oligodendrogloma and glioblastoma paraffin-embedded tissues were prepared from bioptic samples surgically removed from patients who gave

informed consent to the study, kindly provided by Prof. Felice Giangaspero (I.N.M., Neuromed, Pozzilli, Italy). Brain tumor tissues were grouped according to the malignancy, in grade I, II, III, IV. Normal human astrocytes (NHA) (Cambrex, Berkshire, UK), used within 10 passages to avoid biological responsiveness and function deterioration, were grown in Astrocyte Growth Media System (Cambrex). Normal human neural progenitor cells (NHNPC) were purchased from Cambrex and maintained in neural progenitor medium (Cambrex). Primary glioblastoma cell lines FLS and FC1, were prepared from bioptic samples surgically removed from patients who gave informed consent to the study. Samples are available at the human glioma bank Istituto Neurologico Mediterraneo Neuromed. After mechanical dissociation, single cells were resuspended in F10 medium and centrifuged at 1000 g for 5 min. The pellet was resuspended in F10 growth medium supplemented with 10% fetal calf serum (FCS) (Life Technologies Ltd, Milan, Italy), and cells were plated on Petri dishes (Falcon Primaria, Franklin Lakes, NJ, USA) changing the culture medium every 3 days.

The astrocytoma–glioblastoma cell lines U87 (grade III–IV) and U373 (grade III), obtained from the American Type Culture Collection (LGC Promochem, Teddington, UK), were maintained in Dulbecco's modified Eagle's medium supplemented with 10% heat inactivated FCS, 2 mmol/L L-glutamine, 100 IU/mL penicillin, 100 µg streptomycin at 37°C, 5% CO₂ and 95% of humidity.

Human peripheral blood mononuclear cells (PBMC) from normal donors (Blood Bank, ASUR 9, Macerata) were isolated by centrifugation on Ficoll-Hypaque (Lymphoprep, Nicamed, Oslo, Norway) gradient, washed twice, counted and finally resuspended at the appropriate concentration in RPMI 1640 supplemented with 10% FCS, 2 mmol/L L-glutamine, 100 IU/mL penicillin, 100 µg streptomycin.

Materials

The following polyclonal Abs were used: goat anti-human TRPV1 and rabbit anti-human extracellular signal-regulated protein kinase (ERK) from Santa Cruz Biotechnology, Santa Cruz, CA, USA; rabbit anti-human TRPV1 from Chemicon International, Temecula, CA, USA; rabbit anti-human p38 and rabbit anti-human phospho-p38 from Cell Signalling, Beverly, MA, USA; rabbit anti-human caspase 3 (Calbiochem-Novabiochem Corporation, San Diego, CA, USA). Mouse anti-human phospho-ERK monoclonal antibody (mAb) was purchased from Santa Cruz Biotechnology and mouse anti-human α tubulin mAb was obtained from Chemicon International. Horseradish peroxidase (HRP)-conjugated rabbit anti-goat (RAG) from Biomeda Corporation, Foster City, CA, USA; HRP-conjugated donkey anti-rabbit and HRP-conjugated sheep anti-mouse from Amersham Life Sciences, Piscataway, NJ, USA; goat serum (Cappel Research, Durham, NC, USA) was used as negative control. Fluorescein isothiocyanate (FITC)-conjugated annexin V was purchased from MedSystems, Wien, Austria; 5,5',6,6'-tetrachloro-1,1',3,3'-tetraethylbenzimidazolylcarbocyanine iodide (JC-1), propidium iodide (PI) and FLUO 3-AM from Molecular Probes, Leiden, The Netherlands. CPS (*N*-(4-hydroxy-3-methoxy-phenyl)methyl]-8-methyl-6-nonenamide), capsazepine (CPZ) (*N*-[2-(4-chlorophenyl)ethyl]-1,3,4,5-tetrahydro-7,8-dihydroxy-2H-2-benzazepine-2 carbothioamide), [3-(4,5-dimethylthiazol-2-yl)-2,5-diphenyltetrazolium bromide] (MTT), ionomycin, manganese, EDTA, cyclosporine A (CSA), from Sigma-

Aldrich, Milan, Italy. SB203580 and PD98059, specific p38 and ERK inhibitors, respectively, were from Tocris Bioscience, Bristol, UK.

RNA isolation and reverse transcription

Total RNA from fixed paraffin-embedded tissue slices (5–7 μm thick) was isolated by OptimumTM FFPE RNA isolation kit according to the instructions provided (Ambion, Austin, TX, USA). RNA from tumor-free EB was used as non-tumoral tissue control.

Total RNA was extracted from NHA, NHNPC, FLS, FC1, U87 and U373 cell lines using RNeasy Mini kit (Qiagen, Valencia, CA, USA). Cultured cells were first collected by centrifugation for 5 min at 5000 *g*, washed in phosphate-buffered saline (PBS) for 5 min at 5000 *g* and then processed for total RNA extraction following RNeasy protocol instruction.

All RNA samples were dried, resuspended in RNase-free water (Sigma) and their concentration and purity were evaluated by $A_{260\text{ nm}}$ measurement. Two micrograms of RNA extracted from each sample were subjected to reverse transcription in a total volume of 50 μL using the High-Capacity cDNA Archive Kit (RT buffer, dNTP mixture, Random Primers, MultiScribe RT, RNase inhibitor; Applied Biosystems, Foster City, CA, USA). The RT mixtures were incubated for 10 min at 25°C, 2 h at 37°C and finally for 10 min at 75°C. In all, 2 μL of the resulting cDNA products were used as template for real time PCR quantification.

Quantitative real time PCR

Quantitative real time PCR was performed using a IQ5 Multicolor Real time PCR Detection system (Bio-Rad, Hercules, CA, USA) and the reaction mixture contained the Taqman Universal PCR Master Mix (Applied Biosystems) and primer and probe sets. Human TRPV1 primers and probe were purchased as *assay on demand* by Applied Biosystems, cod. Hs00218912_m1. Primers and probe of β -actin, used as housekeeping gene for all real-time PCR performed, were designed by Primer Express and purchased from Sigma Genosys (Sigma-Aldrich). β -actin primers and probe sequence: 5'-CTGGAACGGTGAAGGTGACA (forward); 5'-CGGCCACATTGTGAACCTTTG (reverse); CAGTCGGTTGGAG-CGAGCATCCC (probe).

Each PCR amplification consisted of heat activation for 2 min at 50°C and for 10 min at 95°C followed by 40 cycles of 95°C for 10 s and 60°C for 1 min. All samples were assayed in triplicate in the same plate. Measurement of β -actin levels on the samples was used to normalize mRNA contents and TRPV1 levels were expressed as relative fold of the corresponding control. Statistical analysis was carried out on all the Taqman PCR data.

The analysis of relative quantification of TRPV1 gene expression was calculated as: (i) the mean C_T value of the three replicate wells run for each sample, (ii) the difference (ΔC_T) between the mean C_T value of TRPV1 and C_T value of β -actin, (iii) the difference ($\Delta\Delta C_T$) between the ΔC_T value of the samples and the ΔC_T value of the control chosen (calibrator). The relative quantification value was expressed as $2^{-\Delta\Delta C_T}$.

Immunofluorescence and fluorescent-activated cell sorter analysis

To determine the expression of TRPV1, 5×10^5 NHA, and U87 and U373 glioma cells were fixed and permeabilized using CytoFix/CytoPerm Plus (BD Biosciences, San José, CA, USA) before the

addition of anti-TRPV1 polyclonal Ab directed against a peptide mapping near the carboxy terminus of human protein (1 : 25). Normal goat serum was used as negative control. After 30 min at 4°C, cells were washed twice and labeled with FITC-conjugated RAG (1 : 20). The percentage of positive cells determined over 10 000 events was analyzed on a FACScan cytofluorimeter (Becton-Dickinson, San José, CA, USA) and fluorescent intensity is expressed in arbitrary units on a logarithmic scale.

Confocal laser scanning microscopy analysis

Two $\times 10^5/\text{mL}$ NHA, and U87 and U373 glioma cells, grown for 24 h at 37°C and 5% CO_2 in poly-L-lysine coated slides, were permeabilized using 2% of paraformaldehyde with 0.5% of Triton X-100 in PBS and fixed by 4% of paraformaldehyde in PBS. After three washes in PBS, cells were incubated with 3% of bovine serum albumin and 0.1% of Tween-20 in PBS for 1 h at 20°C and then with a goat anti-TRPV1 (1 : 50) at 4°C overnight. Samples were finally washed with 0.3% of Triton X-100 in PBS three times, incubated with FITC-conjugated RAG Ab (1 : 100) for 1 h at 4°C, mounted and analyzed with MRC600 confocal laser scanning microscope (Bio-Rad) equipped with a Diaphot-TMD (Nikon, Tokyo, Japan) inverted microscope. Fluorochrome was excited with the 600 line of an argon-krypton laser and imaged using a 488-nm (FITC) bandpass filter. Serial optical sections were taken at 1- μm intervals through the cells. Images were processed using Jasc Paint Shop Pro (Corel Corporation, Ottawa, ON, Canada).

Immunohistochemistry

Brain tissues from human epileptic, and glioma biopsies were histologically graded accordingly to the WHO classification criteria. After 20 min of permeabilization in 0.1 mol/L PBS with 0.5% Triton X-100, formalin-fixed, paraffin embedded sections were treated with H_2O_2 for 30 min and incubated for 1 h in 0.1 mol/L PBS solution containing 3% bovine serum albumin and 0.5% Triton X-100. Tissue sections were then incubated overnight at 4°C with a rabbit anti-TRPV1 polyclonal Ab (1 : 1000). Antibody detection was performed by using a multilink streptavidin-biotin complex method (ABC Elite Kit; Vinci Biochem, Vinci, Italy), and Ab was visualized by a diaminobenzidine chromagen method (Sigma Fast 3,3'-diaminobenzidine; Sigma Aldrich, St. Louis, MO, USA). Then, the sections were counter-stained with hematoxylin for nuclei labeling, dehydrated and mounted. The staining intensity of TRPV1 in various gliomas with different grades was determined randomly in four random fields (1 cm^2 each) of each section under 20x magnification by using the Olympus BX51 Microscope and the Image J Software (National Institute of Health).

Western blot analysis

Lysates obtained from NHA, U87 and U373 glioma cells and PBMC, used as positive control, were resuspended in 0.2 mL of lysis buffer (10 mmol/L Tris, pH 7.4, 100 mmol/L NaCl, 1 mmol/L EDTA, 1 mmol/L EGTA, 1 mmol/L NaF, 20 mmol/L $\text{Na}_4\text{P}_2\text{O}_7$, 2 mmol/L Na_3VO_4 , 1% Triton X-100, 10% glycerol, 0.1% sodium dodecyl sulfate (SDS), 0.5% deoxycholate, 1 mmol/L phenylmethylsulfonyl fluoride and protease inhibitor cocktail from Sigma). Samples were separated on 7.5% SDS-polyacrylamide gel, transferred onto Immobilon-P membranes (Millipore, Bedford, MA, USA), and blotted with goat anti-TRPV1 polyclonal Ab (1 : 400)

followed by the incubation with HRP-conjugated RAG (1 : 20 000). In some experiments, lysates from untreated (time zero), CPS (50 $\mu\text{mol/L}$)- and CPS plus CPZ (1 $\mu\text{mol/L}$)-treated U373 glioma cells at different times (8 and 24 h) were separated on 12% sodium dodecyl sulfate–polyacrylamide gel electrophoresis (SDS–PAGE) and immunoblotted with a rabbit polyclonal anti-caspase 3 followed by HRP-conjugated donkey anti-rabbit Ab (1 : 10 000). Each sample was compared with its control (α tubulin) for the purpose of quantification. To evaluate the ability of TRPV1 to trigger MAP kinase activation, lysates obtained from U373 and U87 glioma cells were treated for different times (0, 5, 15, 30 and 60 min) with CPS (50 $\mu\text{mol/L}$) alone or in combination with CPZ (1 $\mu\text{mol/L}$), separated on 9% SDS–PAGE, and immunoblotted with anti-phospho-p38, and anti-p38 MAP kinase or anti-ERK2 (K-23) rabbit polyclonal Ab used as loading controls, followed by HRP-conjugated donkey anti-rabbit (1 : 10 000) Ab, or with a mouse anti-phospho-ERK (E-4) mAb followed by HRP-conjugated sheep anti-mouse (1 : 10 000) Ab. Immunoreactivity was detected using the enhanced chemiluminescence (Amersham Biosciences, Piscataway, NJ, USA), the Chemidoc and Quantity One software (Bio-Rad). Densitometric analysis was performed by using Quantity One software.

[Ca²⁺]_i measurement

Intracellular Ca²⁺ flux was measured as described with some modifications (Amantini *et al.* 2004). Briefly, 4 × 10⁶/mL U87 and U373 glioma cells, were washed in calcium and magnesium free PBS supplemented with 4.5 g/L of glucose. Cells were then resuspended in calcium and magnesium free PBS/glucose medium supplemented with 7 $\mu\text{mol/L}$ FLUO 3-AM and 1 $\mu\text{g/mL}$ Pluronic F-127 (Molecular Probes), dissolved in dimethylsulfoxide, and incubated in the dark for 30 min at 37 °C, 5% CO₂. After washing, cells resuspended in calcium and magnesium free PBS/glucose medium containing 2 mmol/L Ca²⁺ warmed at 37°C, were stimulated with different doses of CPS (1, 10 and 50 $\mu\text{mol/L}$), or with vehicle for different times. In some experiments, glioma cells loaded as above described were treated with CPS (50 $\mu\text{mol/L}$) in combination with CPZ (1 $\mu\text{mol/L}$), or with EDTA (5 mmol/L). FLUO 3-AM fluorescence was measured on the flow cytometer at 525 nm on the green channel; unstimulated cells were analyzed for 2 min to establish baseline fluorescence levels.

MTT assay

The colorimetric MTT survival assay that measures the mitochondrial conversion of the tetrazolium salt to a blue formazan salt, was used to evaluate the viability of CPS-treated glioma cells. Briefly, 2 × 10³ U87 and U373 glioma cells, treated for 24 h at 37°C and 95% of humidity with different doses of CPS (1, 10 and 50 $\mu\text{mol/L}$) or with vehicle in a 96-well microtiter plates, were incubated for the last 3 h with 20 $\mu\text{L/well}$ of MTT (5 mg/mL). Then supernatants were discarded and colored formazan crystals, dissolved with 100 $\mu\text{L/well}$ of dimethylsulfoxide, were read by an ELISA reader (BioTek Instruments, Inc., Winooski, VT, USA).

DNA content analysis

Two × 10⁵/mL U373 glioma cells were grown with or without CPS (50 $\mu\text{mol/L}$) for 24 h at 37°C and 5% CO₂. After washing in PBS, cells were fixed for 30 min on ice by adding 1 mL of 70% cold

ethanol, centrifuged to discard ethanol, stained for 15 min at 20°C with 20 $\mu\text{g/mL}$ PI in DNase-free PBS, and finally analyzed by flow cytometry. The percentage of positive cells determined over 10 000 events was analyzed on a FACScan cytofluorimeter using the CellQuest software (Becton-Dickinson). Fluorescent intensity is expressed in arbitrary units on a logarithmic scale. In some experiments, glioma cells were treated with CPS in combination with CPZ (1 $\mu\text{mol/L}$), or with EDTA (5 mmol/L) or with different doses of SB203580 (50 and 500 nmol/L) or PD98509 (10 and 50 $\mu\text{mol/L}$) inhibitor.

Annexin-V staining

Phosphatidylserine (PS) exposure on U373 glioma cells was detected by annexin V staining and cytofluorimetric analysis. Briefly, 2 × 10⁵/mL glioma cells were treated with CPS (50 $\mu\text{mol/L}$) alone or in combination with CPZ (1 $\mu\text{mol/L}$) for 24 h at 37°C, 5% CO₂, in a 24-well plate. After treatment, cells were washed once with binding buffer (10 mmol/L Hepes/NaOH, pH 7.4, 140 mmol/L NaCl, 2.5 mmol/L CaCl₂) and then stained with 5 μL of annexin V-FITC for 10 min at 20°C. Samples were analyzed by a FACScan cytofluorimeter using the CellQuest software.

Mitochondrial transmembrane potential

Mitochondrial transmembrane potential ($\Delta\Psi_m$) was evaluated by JC-1 staining. JC-1 is a membrane potential-sensitive probe that accumulates in energized mitochondria and subsequent forms J-aggregate from monomers. In apoptotic cells drop of $\Delta\Psi_m$ decreases the J-aggregate emission at 590 nm (red fluorescence) and increases the monomer emission at 530 nm, (green fluorescence). Briefly, 2 × 10⁵/mL U373 glioma cells, resuspended in Dulbecco's modified Eagle's medium/FCS were treated with CPS (50 $\mu\text{mol/L}$) for different times (0, 8 and 24 h) at 37°C and 5% CO₂, incubated 10 min at 20°C with 300 μL of 10 $\mu\text{g/mL}$ JC-1 and analyzed by FACScan cytofluorimeter.

In some experiments, U373 cells were treated for 24 h with CPS (50 $\mu\text{mol/L}$) in combination with CPZ (1 $\mu\text{mol/L}$), or with EDTA (5 mmol/L) or with CSA (1 $\mu\text{mol/L}$) and then loaded as above described. JC-1 was excited by an argon laser (488 nm) and green (530 nm)/red (590 nm) emission fluorescence was collected simultaneously. The carbonyl cyanide chlorophenylhydrazone protonophore, a mitochondrial uncoupler that collapses $\Delta\Psi_m$ was used as positive control. Data were analyzed using the Cell Quest Software.

Statistical analysis

The statistical significance was determined by Student's *t*-test at $p < 0.01$.

Results

Expression of TRPV1 mRNA and protein on glioma cell lines and normal astrocytes

We initially determined the expression of TRPV1 mRNA levels in U87 and U373 glioma cells of astrocytic origin, FC1 and FLS primary glioblastoma cell lines as well as in NHA and NHNPC, by quantitative RT-PCR analysis; we found that TRPV1 mRNA expression was slightly higher in U373

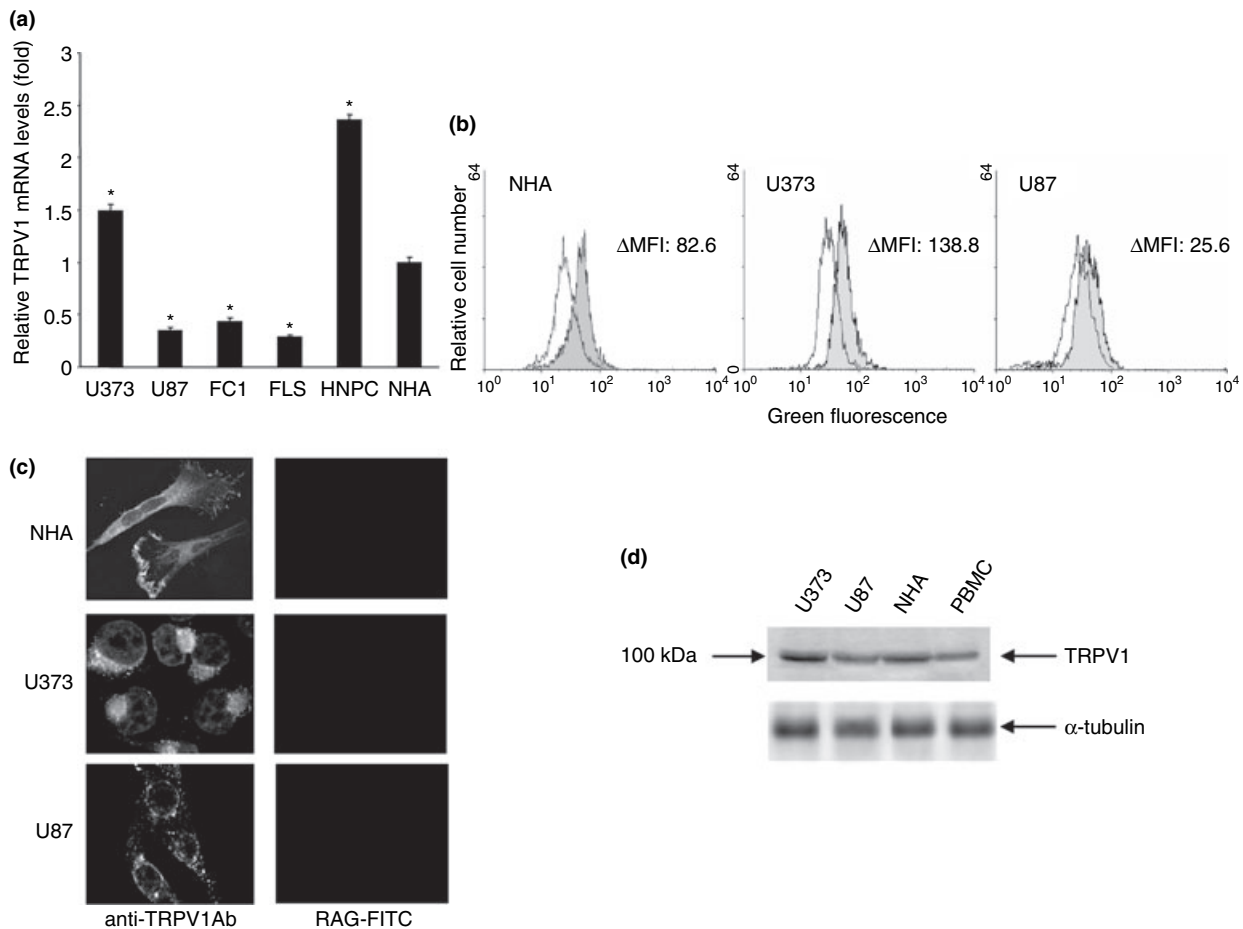


Fig. 1 Expression of transient receptor potential vanilloid type-1 (TRPV1) on glioma cell lines, normal astrocytes and neural progenitor cells. (a) TRPV1 mRNA levels on FLS, FC1, U87 and U373 glioma cell lines and on normal human astrocytes (NHA) and normal human neural progenitor cells (NHNPC) were evaluated by quantitative RT-PCR assayed in triplicate; results (mean \pm SD) are normalized for β -actin expression. TRPV1 levels were expressed as relative fold with respect to NHA used as control. Data shown are representative of three separate experiments. Statistical analysis was performed comparing FLS, FC1, U87, U373, and NHA by Student's *t*-test, ($*p < 0.01$). (b) The expression of TRPV1 on NHA, and U87 and U373 glioma cell lines was evaluated by immunofluorescence and FACS analysis using a goat anti-human TRPV1 polyclonal antibody (Ab). Fluorescein isothiocyanate (FITC)-conjugated rabbit anti-goat (RAG) was used as secondary antibody. The data shown are representative of three separate experiments and are expressed as mean fluores-

cence intensity (Δ MFI) by subtracting the MFI of the secondary antibody to TRPV1 MFI value. White area indicates negative control. (c) Immunocytochemical localization of TRPV1 on NHA, and U87 and U373 glioma cells as evaluated by confocal microscopy. Goat anti-human TRPV1 polyclonal Ab and FITC-conjugated RAG were used as primary and secondary Ab, respectively. Each image is the sum of one of three single optical sections taken at 1- μ m/L intervals. Data shown are representative of three separate experiments. (d) Lysates from U87 and U373 glioma cells, and NHA and peripheral blood mononuclear cells (PBMC) used as controls, were separated on 7.5% sodium dodecyl sulfate-polyacrylamide gel electrophoresis (SDS-PAGE) and probed with a goat anti-human TRPV1 polyclonal Ab. Sizes are shown in kDa and arrowhead indicates the band corresponding to TRPV1. α tubulin levels were evaluated as loading control. Data shown are representative of one of three separate experiments.

cells (1.5-fold) and significantly reduced (about threefold, fourfold and 2.5-fold) in U87, FLS and FC1 cell lines as compared with NHA (Fig. 1a). The expression of TRPV1 on NHA, and U87 and U373 glioma cells was also assessed at protein level. Immunofluorescence and fluorescent-activated cell sorter analysis indicate that a substantial portion of NHA and U373 cells express high levels of TRPV1 [mean fluorescence intensity (Δ MFI) = 82.6

and 138.8, respectively], whereas lower TRPV1 expression (Δ MFI = 25.6) was observed in U87 cells (Fig. 1b). As shown by confocal microscopy analysis, TRPV1 localizes in the cytoplasm and astrocyte processes of NHA cells (Fig. 1c, higher panel), and in discrete spots in the cytoplasmic and perinuclear regions of U87 cells, whereas a clustered distribution was observed on the plasma membrane of U373 cells (Fig. 1c, middle and lower panels, respectively).

Histological type	Grade	No. of cases		Mean relative ^a TRPV1 fold expression
Epileptic brain		8	8/8 (100%)	Negative
Pilocytic astrocytoma	I	13	3/13 (23.1%)	1.44 ± 0.16
			7/13 (53.8%)	0.63 ± 0.09
			3/13 (23.1%)	Negative
Oligodendroglioma	II	6	6/6 (100%)	0.62 ± 0.08
Oligoastrocytoma	II	6	4/6 (66.6%)	0.45 ± 0.07
			2/6 (33.4%)	Negative
Diffuse astrocytoma	II	4	4/4 (100%)	1.47 ± 0.11
Anaplastic oligodendroglioma	III	12	5/12 (41.7%)	0.62 ± 0.08
			7/12 (58.3%)	Negative
Anaplastic astrocytoma	III	5	5/5 (100%)	0.51 ± 0.08
Glioblastoma	IV	14	13/14 (92.8%)	Negative
			1/14 (7.2%)	6.4 ± ND ^b

^aData are represented as mean relative TRPV1 fold expression ± SD of three separate RT-PCR performed in triplicate, normalized to the housekeeping gene (β -actin) and relative to the NHA as control. ^bData are the mean ± SD of three separate RT-PCR performed in triplicate. Numbers in brackets represent the numbers and the percent of the specimens classified according to the TRPV1 expression by quantitative RT-PCR. Formalin-fixed paraffin-embedded brain tissues from human epileptic ($n = 8$), and tumor biopsies ($n = 60$), histologically graded accordingly to the World Health Organization classification criteria, were analyzed for TRPV1 RNA expression by quantitative RT-PCR. TRPV1, transient receptor potential vanilloid type-1; ND, not done.

Western blot analysis of lysates from U87 and U373 cells as well as NHA, revealed a band with apparent MW of 95 kDa likely corresponding to the vanilloid receptor TRPV1, as a similar band was also evident in PBMC used as positive control (Fig. 1d). No reactivity was observed with normal goat serum used as negative control (data not shown).

Loss of TRPV1 mRNA and protein expression in high-grade human malignant glioblastoma

The results obtained with glioblastoma cell lines prompted us to evaluate the expression of TRPV1 mRNA in glioma tissues ($n = 60$) with different grades of malignancy (grade I, II, III and IV) (Table 1) by using quantitative RT-PCR. Total RNA from NHA and tumor-free EB tissues ($n = 8$) were used as positive and negative control, respectively. Our results indicate that irrespective of histotype (astrocytomas and oligodendrogliomas), the levels of TRPV1 expression inversely correlate with the grade of malignancy (Table 1). TRPV1 mRNA was expressed at higher levels on 100% of II grade diffuse astrocytoma, at lower levels on 100% of grade III anaplastic astrocytoma, and was undetectable on 93% of grade IV glioblastomas. Similarly, TRPV1 mRNA was detected on 100% of II grade oligodendroglioma but on only 42% of grade III anaplastic oligodendroglioma. With regard to grade I pilocytic astrocytoma which are clinical and genetically distinct from both diffuse astrocytoma and glioblastoma (Kleihues *et al.* 2000), TRPV1 mRNA expression was rather heterogeneous and a correlation with tumor grade could not be clearly defined. As previously reported no TRPV1 expression was detected in EB tissues (Contassot *et al.* 2004).

Table 1 TRPV1 expression is reduced in human glioma tissues in relation to the grade of malignancy

Transient receptor potential vanilloid type-1 gene expression was also investigated in gliomas of different grades by immunohistochemical analysis (Table 2 and Fig. 2). Consistent with RT-PCR analysis, TRPV1 staining of grade I pilocytic astrocytoma showed a strong immunoreactivity in three of 13 (23.1%), moderate immunoreactivity in seven of 13 (53.8%) and no immunoreactivity in three of 13 (23.1%) specimens analyzed. Grade II oligodendroglioma showed moderate immunoreactivity in six of six (100%), whereas low immunoreactivity in three of six (50%), and no immunoreactivity in three of six (50%) was found in grade II oligoastrocytoma; four of four (100%) of grade II diffuse astrocytoma showed a strong immunoreactivity, with more than 5% of tumor cells being TRPV1 positive (data not shown). No immunoreactivity was evidenced in grade III anaplastic oligodendroglioma (12 of 12) and anaplastic astrocytoma (five of five), grade IV glioblastoma (13 of 13) and tumor-free EB tissues (eight of eight).

Negative control samples were incubated only with the secondary Ab (data not shown). In conclusion, loss of TRPV1 mRNA and protein expression in high-grade glioblastomas suggests that TRPV1 may negatively control tumor progression.

CPS triggers TRPV1-dependent Ca^{2+} influx in U87 and U373 glioma cells

Stimulation of endogenous TRPV1 on neuronal cells (Bevan *et al.* 1992; Dedov *et al.* 2001) by CPS results in an influx of Ca^{2+} , which is inhibited by the specific TRPV1 antagonist, CPZ (Bevan *et al.* 1992).

Table 2 Tumor type and intensity of immunostaining for TRPV1 in tumor-free epileptic and glioma tissues

Tumor type	Grade	No. of cases	Positive cases	Positive rate (%)	Score of TRPV1 expression			
					0	1	2	3
Epileptic brain		8	0	0	8	0	0	0
Pylocytic astrocytoma	I	13	10	77	3	0	7	3
Oligodendroglioma	II	6	6	100	0	0	6	0
Oligoastrocytoma	II	6	3	50	3	3	0	0
Diffuse astrocytoma	II	4	4	100	0	0	0	4
Anaplastic oligodendroglioma	III	12	0	0	12	0	0	0
Anaplastic astrocytoma	III	5	0	0	5	0	0	0
Glioblastoma	IV	13	0	0	13	0	0	0

Formalin-fixed, paraffin-embedded brain tissues from human epileptic, and tumor biopsies, histologically graded accordingly to the World Health Organization classification criteria, were stained with the rabbit anti-TRPV1 polyclonal Ab and analyzed by immunohistochemistry. Intensity of immunoreactivity was evaluated using a semiquantitative scale: score 0 = no staining, or same of background, 1+ = weak staining, 2+ = moderate staining and 3+ = strong staining. TRPV1, transient receptor potential vanilloid type-1.

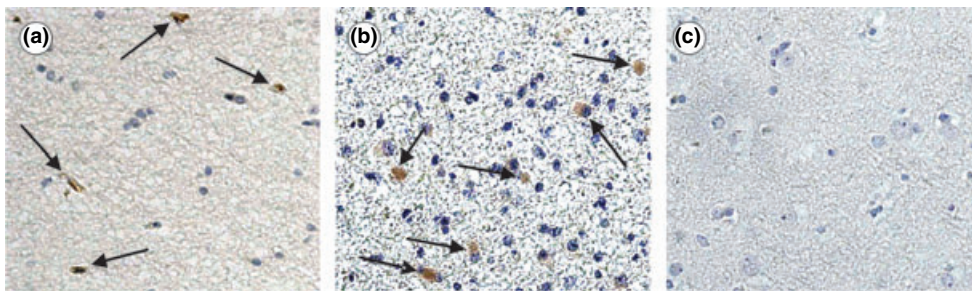


Fig. 2 Immunohistochemical analysis of transient receptor potential vanilloid type-1 (TRPV1) protein in human epileptic and glioma tissues. Shown are representative fields of formalin-fixed, paraffin-embedded brain tissues from human grade I pylocytic astrocytoma (a),

grade II diffuse astrocytoma (b), and grade IV glioblastoma (c) stained with the rabbit anti-TRPV1 polyclonal antibody (Ab). Arrows indicate TRPV1 positive cells. Magnifications, x20.

Thus, to characterize calcium transport through the TRPV1 channel in glioma cells, we evaluated CPS-induced Ca^{2+} influx by flow cytometry in U373 and U87 cells loaded with FLUO-3. CPS stimulation of U373 cells in Ca^{2+} -containing medium resulted in a dose-dependent rise of $[Ca^{2+}]_i$ from 338 to 2252 nmol/L (sevenfold increase at 50 μ mol/L CPS dose) (Fig. 3a), whereas a lower increase (from 260 to 380 nmol/L) was observed in CPS-treated U87 cells (Fig. 3b). Time course analysis of $[Ca^{2+}]_i$ mobilization showed that CPS induces an early response which peaks at 5 s after CPS stimulation, and rapidly (within 60 s) declines to basal levels.

Moreover, by stimulating glioma cells with 50 μ mol/L CPS in the presence of the extracellular calcium chelator EDTA, we found that CPS-induced $[Ca^{2+}]_i$ mobilization was completely blocked, both in U373 and U87 cells. In addition, we found that CPS-induced calcium response in U373 and U87 cells was mediated by TRPV1 as shown by its abrogation by the simultaneous treatment with the CPZ antagonist (Figs 3c and d). Taken together, these results indicate that CPS induces a strong ligand-gated Ca^{2+} influx that is mediated by TRPV1, in U373 but not in U87 cells.

CPS-induces p38 but not ERK1/2 MAPK activation in U373 glioma cells

Previous evidences indicate that CPS activates p38 MAPK in H-ras breast cancer cells and this activity has been suggested to mediate CPS-induced apoptosis (Kang *et al.* 2003). Thus, we initially evaluated the ability of CPS to activate ERK and p38 MAPKs. To this purpose, U373 and U87 cells were stimulated for different times with 50 μ mol/L CPS, and cell lysates were separated on SDS-PAGE and then immunoblotted with anti-phospho-ERK and anti-phospho-p38 specific Abs. As shown in Fig. 4a, CPS treatment of U373 but not U87 cells induced a time-dependent p38 MAPK activation, which was already evident at 5 min, peaked at 15 min and declined at 60 min after CPS treatment. By contrast, ERK1/2 were phosphorylated at basal level, and CPS treatment did not further increase phosphorylation in both glioma cell lines (Fig. 4a). ERK activation was induced by 12-*O*-tetradecanoylphorbol 13-acetate on U373 cells and used as positive control (data not shown). All lysates contained comparable levels of ERK and p38 proteins, as evaluated by western blot.

Capsaicin-induced p38 MAPK phosphorylation of U373 cells is TRPV1-dependent as shown by the ability of the CPZ

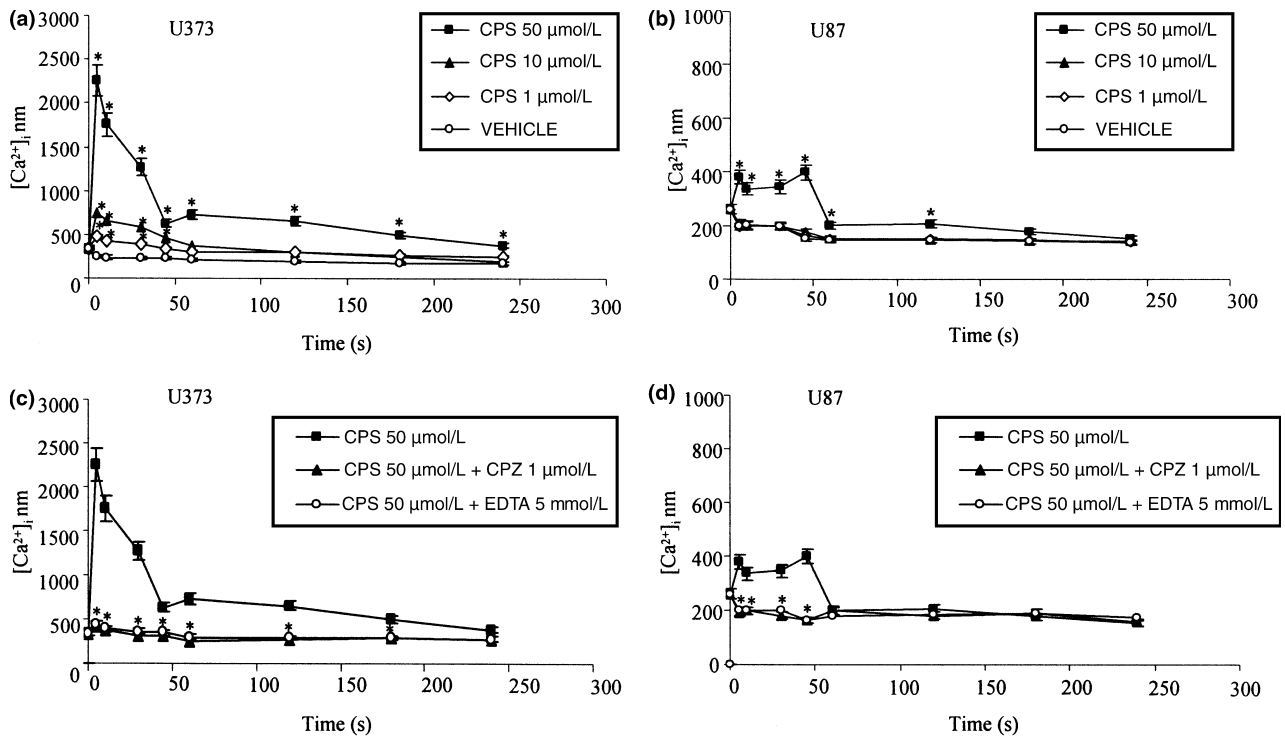


Fig. 3 Triggering of transient receptor potential vanilloid type-1 (TRPV1) on U87 and U373 by capsaicin (CPS) induces calcium influx. (a and b) Time course of intracellular free calcium ($[Ca^{2+}]_i$) rise in FLUO 3-loaded vehicle- or CPS (1, 10 and 50 $\mu\text{mol/L}$)-treated U373 (a) and U87 (b) glioma cells was evaluated at different times by FACS analysis. Data shown are the mean \pm SD of three separate experiments. Statistical analysis was determined by comparing vehicle with CPS-treated glioma cells; * $p < 0.01$ determined by Student's *t*-test.

(c and d) Time course of $[Ca^{2+}]_i$ rise in FLUO 3-loaded CPS (50 $\mu\text{mol/L}$)-, CPS plus capsazepine (CPZ) (10 $\mu\text{mol/L}$)- or CPS plus EDTA (5 mmol/L)-treated U373 (c) and U87 (d) glioma cells was evaluated by cytofluorimetric and FACS analysis as above described. Data shown are the mean \pm SD of three separate experiments. Statistical analysis was determined by comparing CPS- with CPS plus CPZ-, and CPS- with CPS plus EDTA- treated glioma cell lines; * $p < 0.01$ determined by Student's *t*-test.

to completely abrogate the p38 MAPK phosphorylation induced by CPS stimulation (Fig. 4b). Consistent with the calcium response, these results indicate that CPS induces p38 but not ERK activation that is mediated by TRPV1, in U373 but not in U87 cells.

CPS triggers apoptotic cell death in U373 but not U87 glioma cells

Recent findings indicate that *in vitro* CPS treatment can promote apoptosis in different cell types (Hail 2003). Thus, we initially evaluated whether CPS could affect cell viability by MTT assay in glioma cells treated for 24 h with CPS. We found that the percentage of dead U373 cells increased with the increase of CPS dose from 11% in vehicle or 1 $\mu\text{mol/L}$ CPS-treated cells to 28.5% and 88.2% in cells treated with 10 or 50 $\mu\text{mol/L}$ of CPS, respectively (Fig. 5a). On the contrary, U87 cells were resistant to CPS-induced cell death also at higher (300 $\mu\text{mol/L}$) doses (data not shown).

DNA fragmentation during apoptosis leads to extensive loss of DNA content resulting in a distinct sub-G₀/G₁ peak detected by PI staining and flow cytometry. Treatment of U373 cells, but not U87 (data not shown) with CPS

(50 $\mu\text{mol/L}$) resulted in increased hypodiploid DNA content from 10.8% (vehicle treated) to 89.2% (Fig. 5b). Capsaicin-induced DNA fragmentation was TRPV1 dependent, as it was completely reverted by CPZ (Fig. 4b). No cell death was observed when glioma cells were incubated at the same time with the CPS or CPZ vehicle alone (data not shown).

Intracellular calcium flux plays a major role in many pathways leading to apoptotic cell death in several cell types (McConkey and Orrenius 1996; Hail 2003). Thus, we determined the requirement of extracellular calcium in CPS-induced DNA fragmentation of U373 cells. As shown by Fig. 5b, CPS-induced increase of hypodiploid DNA was completely inhibited in the presence of EDTA. Overall, these results indicate that CPS-induced DNA fragmentation in U373 cells is mediated by TRPV1, and requires CPS-induced ligand-gated Ca^{2+} influx.

Once the functional expression of TRPV1 on U373 cells was observed, we analyzed whether the CPS-induced opening of calcium channels could induce externalization of PS residues from the inner to the outer leaflet of the plasma membrane. To this end, we analyzed the annexin V binding on U373 cells by flow cytometry. As shown in

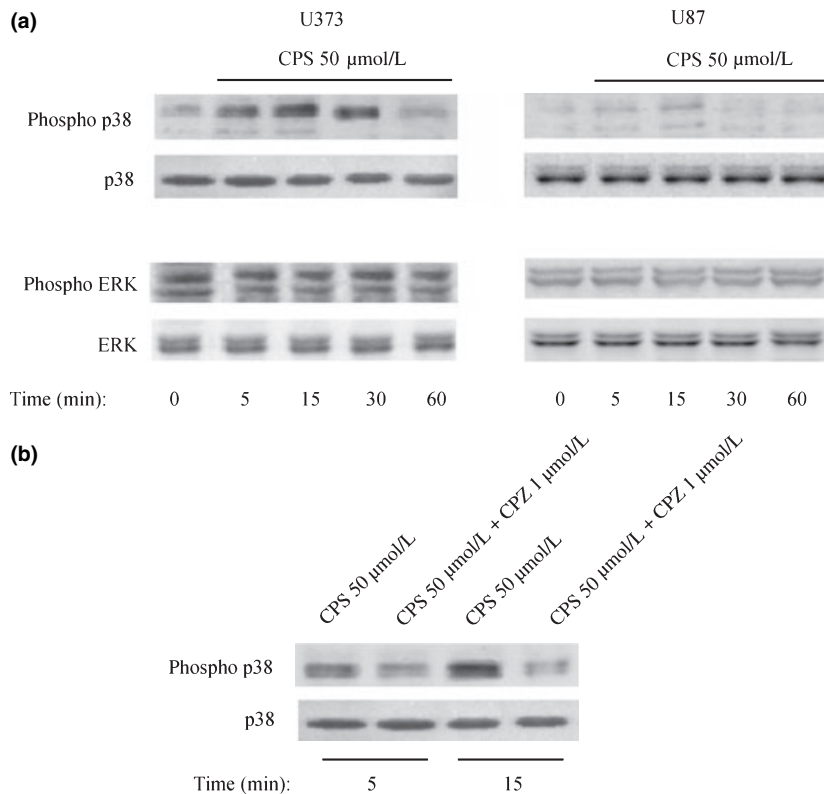


Fig. 4 Capsaicin (CPS) induces transient receptor potential vanilloid type-1 (TRPV1)-dependent p38 but not extracellular signal-regulated protein kinase (ERK) mitogen-activated protein kinase (MAPK) activation. (a) Lysates from CPS (50 μmol/L)-treated U373 or U87 glioma cells for different times (0, 5, 15, 30 and 60 min) were separated on 9% sodium dodecyl sulfate–polyacrylamide gel electrophoresis (SDS–PAGE) and probed with following Abs: rabbit anti-human phospho-p38, mouse anti-human phospho-ERK, rabbit anti-human p38 or rabbit

anti-human ERK. Data are representative of one of three separate experiments. (b) Lysates from U373 glioma cells treated for different times (5 and 15 min) with 50 μmol/L CPS alone or in combination with capsazepine (CPZ) (1 μmol/L) were separated on 9% SDS–PAGE and probed with a rabbit anti-human phospho-p38 and a rabbit anti-human p38. Data are representative of one of three separate experiments.

Fig. 4c, treatment with 50 μmol/L CPS for 24 h induces translocation of PS in about 79% of glioma cells. No increase in PS expression was found in vehicle-treated cells (data not shown). CPS-induced PS exposure on U373 cells was mediated by TRPV1, as was completely inhibited (from 79% to 18%) by CPZ (Fig. 5c); PS expression on U373 cells was not affected by CPZ alone (data not shown).

CPS triggers TRPV1-dependent mitochondrial $\Delta\Psi_m$ dissipation and caspase 3 activation in U373 glioma cells

To understand the involvement of mitochondria in CPS-induced apoptotic cell death, we treated U373 cells at different times (0, 8 and 24 h) with 50 μmol/L CPS, and then labeled with JC-1, and measured $\Delta\Psi_m$ by two color flow cytometry. Treatment with CPS induced a time dependent decrease of red fluorescence and a concomitant increase of green fluorescence intensity (depolarization) (Fig. 6a). CPS-induced $\Delta\Psi_m$ dissipation was evident at 8 h after treatment in about 25.4% of glioma cells and was maximal (80.6%) at 24 h. CPS-induced $\Delta\Psi_m$ dissipation was TRPV1 dependent,

as it was completely reverted by CPZ (Fig. 6b), whereas CPZ alone did not affect the mitochondrial integrity of glioma cells (data not shown).

Capsaicin has been reported to enhance mitochondrial calcium accumulation and opening of the permeability transmembrane pore (PTP). Thus, we analyzed the effect of EDTA and CSA, that can inhibit mitochondrial-damage-induced apoptosis by preventing PTP opening (Kroemer and Reed 2000) on CPS-induced $\Delta\Psi_m$ dissipation. Depletion of extracellular calcium by EDTA, or addition of CSA, completely blocked the ability of CPS to dissipate $\Delta\Psi_m$ (Fig. 6b). Overall, these results suggest that CPS-induced TRPV1-mediated $\Delta\Psi_m$ dissipation in U373 cells involves mitochondrial calcium uptake and PTP opening induced by calcium overload.

Mitochondrion-dependent apoptosis is initiated by recruitment and activation of caspases (Cohen 1997), and caspase activity is associated with vanilloid-induced apoptosis (Hail 2003; Amantini *et al.* 2004). Thus, we analyzed whether caspase 3 was activated during CPS-induced apoptosis of

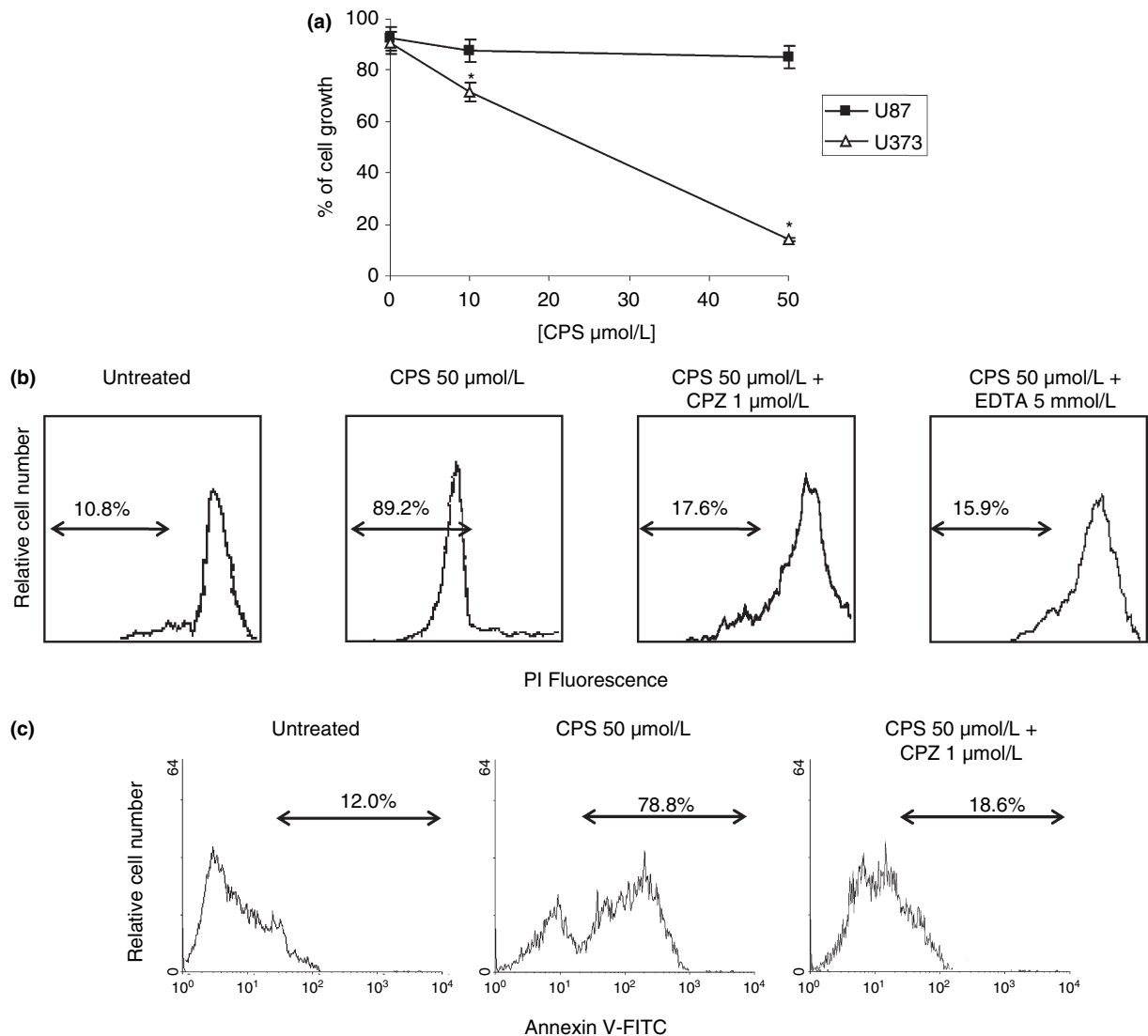


Fig. 5 Capsaicin (CPS) treatment affects cell viability and induces apoptosis in U373, but not U87 glioma cells. (a) Cell growth was evaluated by 3-(4,5-dimethylthiazol-2-yl)-2,5-diphenyltetrazolium bromide (MTT) assay in U373 and U87 glioma cells untreated or treated for 24 h at 37°C, with CPS (1, 10 and 50 $\mu\text{mol/L}$). * $p < 0.01$ determined by Student's *t*-test. (b) CPS-induced DNA fragmentation was assessed in untreated, CPS (50 $\mu\text{mol/L}$)-, CPS plus capsazepine (CPZ) (1 $\mu\text{mol/L}$)- or CPS plus EDTA (5 mmol/L)-treated U373 glioma

cells by propidium iodide (PI) staining and FACS analysis. Numbers indicate the percentage of cells showing hypodiploid peak. Data are representative of one of three separate experiments. (c) The percentage of annexin V⁺ U373 glioma cells untreated or treated for 24 h with CPS (50 $\mu\text{mol/L}$) alone or in combination with CPZ (1 $\mu\text{mol/L}$) was evaluated by immunofluorescence and FACS analysis. Data are representative of one of three different experiments.

U373 cells by monitoring the proteolysis of 32 kDa procaspase 3. CPS (50 $\mu\text{mol/L}$) treatment of U373 cells stimulated the cleavage of procaspase 3 in a time-dependent manner as demonstrated by the appearance of the 17 and 12 kDa caspase 3 active fragments (Fig. 6c). Moreover, treatment of U373 cells with CPS plus CPZ completely inhibited procaspase 3 cleavage, thus indicating that CPS-induced caspase 3 activity is coupled to TRPV1 (Fig. 6c). Overall, our results suggest that CPS-induced glioma cell apoptosis involves TRPV1-dependent activation of caspase 3.

p38 MAPK activation is required for CPS-induced apoptosis of U373 glioma cells

Recently, p38 but not pERK1/2 MAPK activation has been suggested to mediate chemotherapeutic agent-induced apoptosis of different cancer cells (Bradham and McClay 2006). Thus, we determined the ability of MAPK selective inhibitors to affect CPS-induced apoptosis of U373 cells. SB203580, a selective p38 MAPK inhibitor markedly inhibited in a dose-dependent manner the apoptosis of glioma cells induced by CPS (Fig. 7); by contrast, in

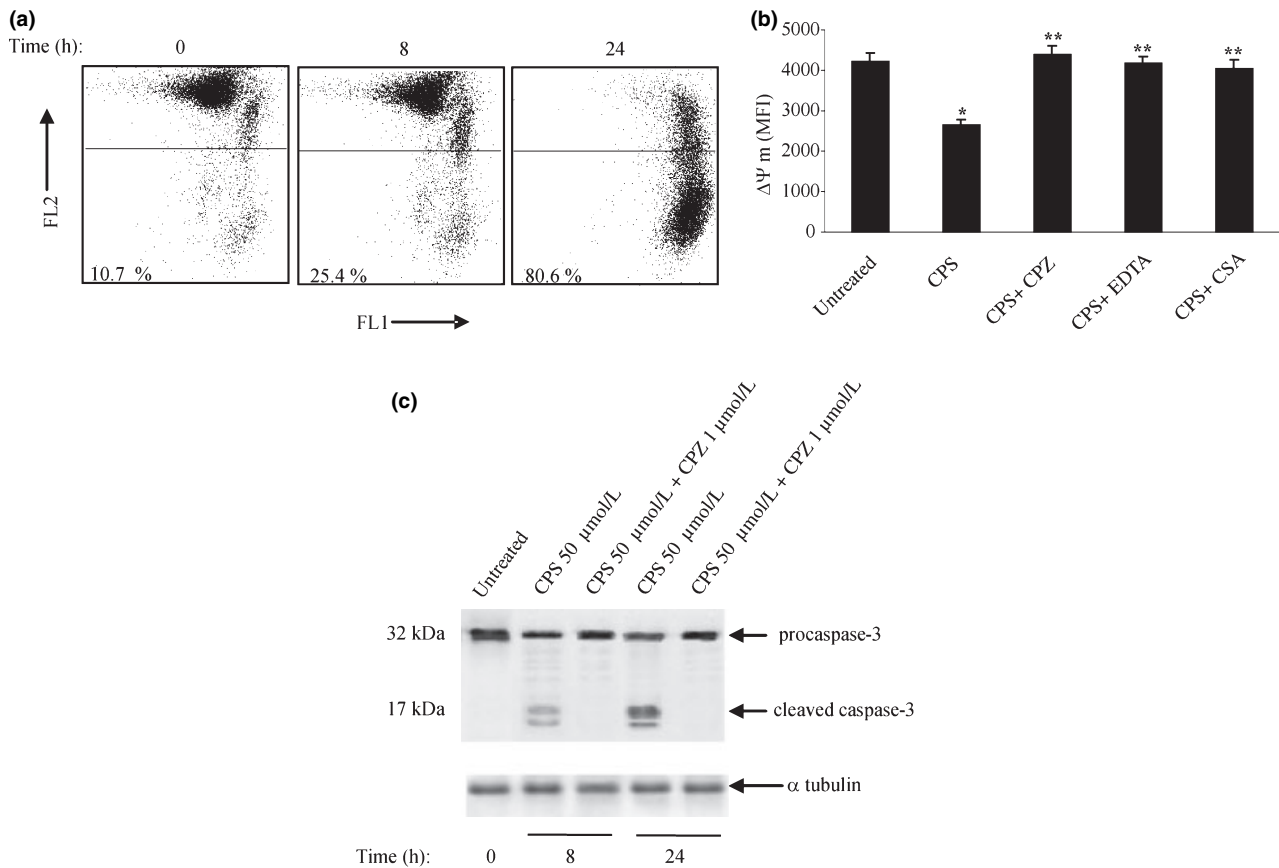


Fig. 6 Capsaicin (CPS) triggers a transient receptor potential vanilloid type-1 (TRPV1)-dependent mitochondrial transmembrane potential ($\Delta\Psi_m$) dissipation and caspase 3 activation in U373 glioma cells. (a) Analysis of $\Delta\Psi_m$ changes on CPS (50 $\mu\text{mol/L}$)-treated U373 glioma cells was evaluated for different times (0, 8 and 24 h) by 5,5',6,6'-tetrachloro-1,1',3,3'-tetraethylbenzimidazolylcarbocyanine iodide (JC-1) staining and biparametric FL1(green)/FL2(red) flow cytometric analysis. Numbers indicate the percentage of cells showing a drop in the $\Delta\Psi_m$ -related red fluorescence intensity. Data are representative of one of three separate experiments. (b) Analysis of $\Delta\Psi_m$ changes on untreated, CPS (50 $\mu\text{mol/L}$ -), CPS plus capsazepine (CPZ) (1 $\mu\text{mol/L}$ -), CPS plus EDTA (5 mmol/L), or on CPS plus cyclosporine A (CSA) (1 $\mu\text{mol/L}$)-treated glioma cells was evaluated as above described.

Data are the mean \pm SD of three separate experiments. Statistical analysis was determined by comparing untreated with CPS-treated ($*p < 0.01$); CPS- with CPS plus CPZ-, CPS plus EDTA, or CPS plus CSA-treated glioma cells ($**p < 0.01$) determined by Student's *t*-test. (c) Lysates from untreated, CPS (50 $\mu\text{mol/L}$)- or CPS plus CPZ (1 $\mu\text{mol/L}$)-treated U373 glioma cells for different times (0, 8 and 24 h) were separated on 12% sodium dodecyl sulfate-polyacrylamide gel electrophoresis (SDS-PAGE) and probed with a rabbit anti-caspase 3 polyclonal antibody (Ab). Sizes are shown in kDa and arrowheads indicate the bands corresponding to procaspase 3 and caspase 3 cleaved fragments. α tubulin levels were evaluated as loading control. Data are representative of one of three separate experiments.

accordance with the failure of CPS to induce ERK activation, PD98509, a selective inhibitor of MEK1, did not show any effect at all the doses used (Fig. 7). Overall, these results demonstrate that p38 but not ERK MAPK activation is required for the induction of TRPV1-dependent apoptosis of U373 cells by CPS.

Discussion

Herein, we provide evidence on the expression of TRPV1 by glioma cell lines and tissues, and its involvement in the apoptotic cell death induced by *in vitro* CPS treatment. As evaluated by quantitative RT-PCR, TRPV1 mRNA was

expressed in a number of tumor cells of astrocytic origin, such as U87 and U373 glioma cells, and FC1 and FLS primary glioblastoma cell lines, with higher expression observed in U373 cells, and in NHA and NHNPC. Moreover, TRPV1 protein expression was assessed on NHA, and U87 and U373 glioma cells by western blot and cytofluorimetric analysis, and paralleled mRNA levels. In addition, TRPV1 was identified as a single band of 95 kDa, likely corresponding to the non-glycosylated form of TRPV1 (Kedei *et al.* 2001). Notably, confocal microscopy analysis indicated that TRPV1 shows a cell type-dependent subcellular localization, with TRPV1 present in the cytoplasm and astrocyte processes of NHA, in discrete spots in the cytoplasmic and

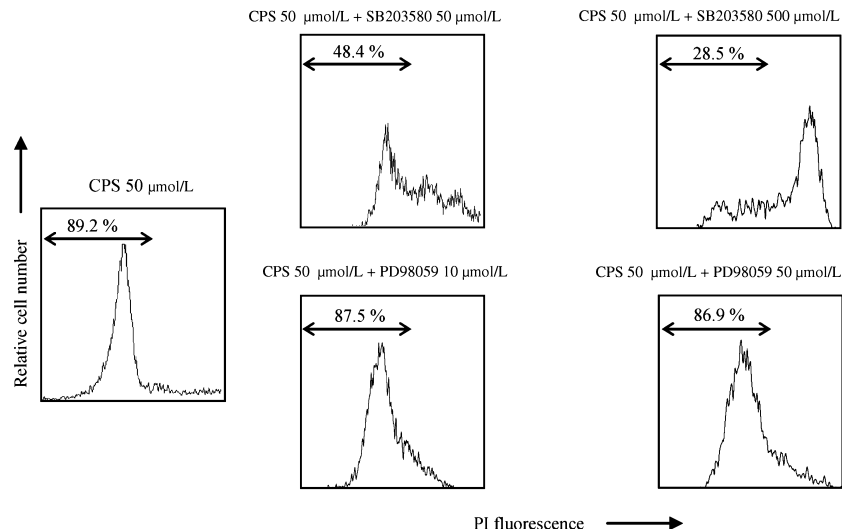


Fig. 7 p38 but not extracellular signal-regulated protein kinase (ERK) mitogen-activated protein kinase (MAPK) activation is required for capsaicin (CPS)-induced apoptosis of U373 glioma cells. DNA fragmentation was evaluated by propidium iodide (PI) staining and FACS analysis in U373 glioma cells treated for 24 h at 37°C with 50 μmol/L

of CPS alone or in combination with different doses of SB203580 (50 and 500 nmol/L) or PD98059 (10 and 50 μmol/L) inhibitor. Numbers indicate the percentage of cells showing hypodiploid peak. Data are representative of one of three separate experiments.

perinuclear regions of U87 cells, and a clustered distribution on the plasma membrane of U373 cells.

We also tested whether TRPV1 gene expression was associated with glioma growth and progression by analyzing 60 glial tumors with different grades of malignancy. Our results indicate that irrespective of histotype (astrocytomas and oligodendrogliomas), TRPV1 expression progressively decreases in high grade (III and IV) gliomas, with a complete loss observed in 93% of grade IV glioblastomas.

Consistent with previous evidence, TRPV1 mRNA expression on tumor-free EB tissues (Contassot *et al.* 2004) was negative. Based on a number of evidence describing increased risk of glioma associated with a history of epilepsy (Schwartzbaum *et al.* 2005), our finding suggests the existence of similar mechanisms regulating TRPV1 gene expression in these brain diseases.

Consistent with TRPV1 expression at mRNA level, a parallel reduction of TRPV1 protein expression is observed by immunohistochemical analysis of glioma tissues, as grade increases. Thus, a complete loss of TRPV1 protein expression was found in grade III anaplastic oligodendroglioma and anaplastic astrocytoma, grade IV glioblastoma. Finally, no TRPV1 protein expression was also found in tumor-free EB tissues.

In attempt to explore the functional role of TRPV1 on glioma cells, we initially analyzed the ability of its synthetic agonist CPS to induce both receptor proximal events such as calcium mobilization and MAPK activation, and apoptosis. Our findings indicate that treatment of U373 cells with CPS induces a rapid rise of $[Ca^{2+}]_i$, which is completely inhibited

by EDTA, and is blocked by CPZ. On the contrary, in accordance with the levels of receptor expression, a moderate TRPV1-dependent increase in $[Ca^{2+}]_i$ was observed in U87 cells. Our results are consistent with previous evidence in a number of different neuronal cell types including dorsal root ganglion and sensory neurons (Bevan *et al.* 1992; Dedov *et al.* 2001), C6 rat glioma cells (Macho *et al.* 1999), and in TRPV1-HEK293 cell transfectants (Grant *et al.* 2002), showing that stimulation of TRPV1 with CPS results in Ca^{2+} influx that is inhibited by CPZ.

Our results provide also evidence that CPS-induced TRPV1 triggering on U373, but not on U87 cells rapidly stimulates p38 but not ERK MAPK activation that is completely inhibited by CPZ. These results are in agreement with previous findings in H-ras breast cancer cells, showing that CPS treatment markedly activates Jun N-terminal protein kinase-1 and p38 MAPKs, while it deactivates ERK MAPKs (Kang *et al.* 2003). However, CPS-induced ERK phosphorylation of sensory neurons (Zhuang *et al.* 2004) has been also reported.

The study of the involvement of TRPV1 in CPS-induced glioma cell apoptosis showed that CPS markedly reduces cell viability and induces DNA fragmentation in U373, but not U87 cells in a TRPV1-dependent manner as shown by the use of CPZ. In accordance with the role of calcium in apoptotic cell death, we observed that depletion of extracellular Ca^{2+} by EDTA prevented CPS-induced oligonucleosomal DNA fragmentation in U373 cells. Our results are consistent with previous evidence showing the TRPV1-dependent stimulation of calcium by CPS in rat glioma cells (Biro *et al.* 1998).

Overall, our findings indicate that the expression of TRPV1 on U373 and U87 cells is functionally linked to calcium mobilization flux and sensitivity to CPS-induced apoptosis. A characteristic feature of apoptotic cell death is the loss of phospholipid asymmetry and the expression of PS on the outer layer of the plasma membrane. Our results show that CPS treatment of U373 cells induces externalization of PS on U373 cells. The involvement of TRPV1 on PS externalization was directly demonstrated by the ability of CPZ to revert this CPS-induced event.

Reduction in mitochondrial potential constitutes an early irreversible step of programmed cell death (Mignotte and Vayssiere 1998). Our study demonstrates that CPS causes an irreversible $\Delta\Psi_m$ dissipation which is completely inhibited by CPZ, indicating that activation of TRPV1 by binding to its specific ligand, triggers the mitochondrion-dependent apoptotic program. In addition, by the use of CSA (Kroemer and Reed 2000), we show the ability of CPS to dissipate $\Delta\Psi_m$ by mitochondrial PTP opening, suggesting that this event plays an important role in CPS-induced apoptotic cell death. Moreover, in accordance with the finding of $[Ca^{2+}]_i$ influx requirement in the CPS-induced apoptosis, we demonstrate by the use of EDTA that Ca^{2+} influx plays a decisive role in the collapse of $\Delta\Psi_m$ upon TRPV1 activation by CPS leading to PTP opening and cell death. Similarly, CSA-mediated inhibition of CPS-induced loss of $\Delta\Psi_m$ was reported in rat thymocytes (Amantini *et al.* 2004).

Our results on the role of mitochondrial permeability transition in CPS-induced apoptosis are further supported by previous evidence indicating that over-expression of Bcl-2 that inhibits PTP, reduces CPS-induced PS exposure (Kroemer and Reed 2000) and blocks CPS-mediated $\Delta\Psi_m$ disruption and apoptosis (Macho *et al.* 1998).

Mitochondrial transmembrane dissipation leading to activation of executioner caspases occurs during apoptosis. Our results indicate that CPS induces a dose-dependent activation of caspase 3, which is completely inhibited by CPZ. Accordingly, increased procaspase 3 cleavage was observed during CPS-induced apoptosis of human hepatocarcinoma cells (Jung *et al.* 2001), H-ras breast cancer cells (Kang *et al.* 2003), and rat thymocytes (Amantini *et al.* 2004). Overall these results demonstrate that CPS through interaction with TRPV1 induces sustained $[Ca^{2+}]_i$ levels and thus triggers PTP opening, mitochondrial damage, activation of caspase 3 and apoptotic cell death in U373 cells.

Based on the evidence that p38 MAPK family plays a central role in the signaling pathways controlling of cell survival and apoptosis (Wada and Penninger 2004), and TRPV1 stimulation by CPS triggers p38 MAPK activation on U373 cells, we analyzed p38 MAPK involvement in CPS-induced apoptosis by the use of specific pharmacological inhibitors. Consistent with the ability of CPS to selectively activate p38 but not ERK MAPK, we found that CPS-induced apoptosis of U373 cells was inhibited in a dose-

dependent manner by p38 (SB203580) but not ERK (PD98509) inhibitor, indicating that p38 but not ERK is involved in the control of TRPV1-mediated glioma apoptotic cell death. In agreement with our findings, p38 MAPK inhibitors, or over-expression of dominant negative forms of Jun N-terminal protein kinase-1 and p38, but not that of ERKs, blocked CPS-induced apoptosis of H-ras breast cancer cells (Kang *et al.* 2003).

Which might be the pathophysiological relevance of TRPV1 expression and pro-apoptotic activity on glioma cell growth and progression? Recent evidence indicate that human glioblastomas express enhanced levels of endogenous TRPV1 ligand(s) such as AEA and *N*-stearoyethanolamine (Petersen *et al.* 2005) that can inhibit cell proliferation and activate apoptosis in a TRPV1-dependent manner (Maccarrone *et al.* 2000; Maccarrone *et al.* 2002). Thus, we can hypothesize that the reduced expression and complete loss of TRPV1 receptor that we found to correlate with tumor progression, may represent a mechanism by which tumor cells can evade antiproliferative and pro-apoptotic signals. In addition, as AEA binds to CB1 and CB2 cannabinoid receptors which exert a protective effect on TRPV1-dependent AEA-induced glioma cell apoptosis (Maccarrone *et al.* 2000; Contassot *et al.* 2004), reduced TRPV1 expression may favor binding of the endocannabinoids to cannabinoid receptors, therefore promoting tumor cell survival.

Thus, we can suggest that molecular profiling of TRPV1 channel in glioma tumors, may represent a valuable tool for glioma prognosis and follow-up, and an efficient target for novel therapeutic approaches.

Acknowledgements

Partially supported by Ministero dell'Università e della Ricerca Scientifica e Tecnologica (MIUR), University of Camerino. We thank Dr Patrizia Ballarini (Department of Molecular, Cellular and Animal Biology, University of Camerino, Camerino, Italy) for confocal microscopy analysis assistance.

References

- Amantini C., Mosca M., Lucciarini R., Perfumi M., Morrone S., Piccoli M. and Santoni G. (2004) Distinct thymocyte subsets express the vanilloid receptor VR1 that mediates capsaicin-induced apoptotic cell death. *Cell Death Differ.* **11**, 1342–1356.
- Bevan S., Hothi S., Hughes G., James I. F., Rang H. P., Shah K., Walpole C. S. and Yeasts J. C. (1992) Capsazepine: a competitive antagonist of the sensory neurone excitant capsaicin. *Br. J. Pharmacol.* **107**, 544–552.
- Biro T., Brodie C., Modarres S., Lewin N. E., Acs P. and Blumberg P. M. (1998) Specific vanilloid responses in C6 rat glioma cells. *Brain Res. Mol.* **56**, 89–98.
- Bradham C. and McClay D. R. (2006) p38 MAPK in development and cancer. *Cell Cycle* **8**, 824–828.
- Caterina M. J. and Julius D. (2001) The vanilloid receptor: a molecular gateway to the pain pathway. *Annu. Rev. Neurosci.* **24**, 487–517.

- Caterina M. J., Schumacher M. A., Tominaga M., Rosen T. A., Levine J. D. and Julius D. (1997) The capsaicin receptor: a heat-activated ion channel in the pain pathway. *Nature* **389**, 816–824.
- Caterina M. J., Leffler A., Malmberg A. B., Martin W. J., Trafton J., Petersen-Zeit K. R., Koltzenburg M., Basbaum A. I. and Julius D. (2000) Impaired nociception and pain sensation in mice lacking the capsaicin receptor. *Science* **288**, 306–313.
- Cohen G. M. (1997) Caspases: the executioners of apoptosis. *Biochem. J.* **326**, 1–15.
- Contassot E., Wilmotte R., Tenan M., Belkouch M. C., Schnuriger V., de Tribolet N., Burkhardt K. and Dietrich Y. (2004) Arachidonyl-ethanolamide induces apoptosis of human glioma cells through vanilloid receptor-1. *J. Neuropathol. Exp. Neurol.* **63**, 956–963.
- Dedov V. N., Mandadi S., Armati P. J. and Verkhratsky A. (2001) Capsaicin-induced depolarisation of mitochondria in dorsal root ganglion neurons is enhanced by vanilloid receptors. *Neuroscience* **103**, 219–226.
- Grant E. R., Dubin A. E., Zhang S. P., Ziviv R. A. and Zhong Z. (2002) Simultaneous intracellular calcium and sodium flux imaging in human vanilloid receptor 1 (VR1)-transfected human embryonic kidney cells: a method to resolve ionic dependence of VR1-mediated cell death. *J. Pharmacol. Exp. Ther.* **300**, 9–17.
- Grossman S. A. and Batarra J. F. (2004) Current management of glioblastoma multiforme. *Semin. Oncol.* **31**, 635–644.
- Gunthorpe M. J., Benham C. D., Randall A. and Davis J. B. (2002) The diversity in the vanilloid (TRPV) receptor family of ion channels. *Trends Pharmacol. Sci.* **23**, 183–191.
- Hail N. Jr. (2003) Mechanisms of vanilloid-induced apoptosis. *Apoptosis* **8**, 251–262.
- Holzer P. (1991) Capsaicin: cellular targets, mechanisms of action, and selectivity for thin sensory neurons. *Pharmacol. Rev.* **43**, 143–201.
- Ito K., Nakazato T., Yamato K., Miyakawa Y., Yamada T., Hozumi N., Segawa K., Ikeda Y. and Kizaki M. (2004) Induction of apoptosis in leukemic cells by homovanillic acid derivative, capsaicin, through oxidative stress: implication of phosphorylation of p53 at Ser-15 residue by reactive oxygen species. *Cancer Res.* **64**, 1071–1078.
- Jung M. Y., Kang H. J. and Moon A. (2001) Capsaicin-induced apoptosis in SK-Hep-1 hepatocarcinoma cells involves Bcl-2 down-regulation and caspase-3 activation. *Cancer Lett.* **165**, 139–145.
- Kang H. J., Soh Y., Kim M. S., Lee E. J., Surh Y. J., Kim H. R., Kim S. H. and Moon A. (2003) Roles of JNK-1 and p38 in selective induction of apoptosis by capsaicin in ras-transformed human breast epithelial cells. *Int. J. Cancer* **103**, 475–482.
- Kedei N., Szabo T., Lile J. D., Treanor J. J., Olah Z., Iadarola M. J. and Blumberg P. M. (2001) Analysis of the native quaternary structure of the vanilloid receptor 1. *J. Biol. Chem.* **276**, 28613–28619.
- Kleihues P., Davis R. L., Ohigaki H., Burger P. C., Westphal M. M. and Cavenee W. K. (2000) Diffuse astrocytoma, in *Pathology and Genetics of Tumors of the Nervous System* (Kleihues P. and Cavenee W. K., eds.), pp. 22–26. IARC Press, Lyon.
- Kleihues P., Louis D. N., Scheithauer B. W., Rorke L. B., Reifenberger G., Burger P. C. and Cavenee W. K. (2002) The WHO classification of tumors of the nervous system. *J. Neuropathol. Exp. Neurol.* **61**, 215–225.
- Kroemer G. and Reed J. C. (2000) Mitochondrial control of cell death. *Nat. Med.* **6**, 513–519.
- Lee Y. S., Nam D. H. and Kim J. A. (2000) Induction of apoptosis by capsaicin in A172 human glioblastoma cells. *Cancer Lett.* **161**, 121–130.
- Maccarrone M., Pauselli R., di Rienzo M. and Finazzi-Agrò A. (2002) Binding, degradation and apoptotic activity of stearyl ethanolamide in rat C6 glioma cells. *Biochem. J.* **366**, 137–144.
- Maccarrone M., Lorenzon T., Bari M., Melino G. and Finazzi-Agrò A. (2000) Anandamide induces apoptosis in human cells via vanilloid receptors. Evidence for a protective role of cannabinoid receptors. *J. Biol. Chem.* **275**, 31938–31945.
- Macho A., Blazquez M. V., Navas P. and Munoz E. (1998) Induction of apoptosis by vanilloid compounds does not require de novo gene transcription and activator protein 1 activity. *Cell Growth Differ.* **9**, 277–286.
- Macho A., Calzado M. A., Munoz-Blanco J., Gomez-Diaz C., Gajate C., Mollinedo F., Navas P. and Munoz E. (1999) Selective induction of apoptosis by capsaicin in transformed cells: the role of reactive oxygen species and calcium. *Cell Death Differ.* **6**, 155–165.
- Maher E. A., Furnari F. B., Bachoo R. M., Rowitch D. H., Louis D. N., Cavenee W. K. and DePinho R. A. (2001) Malignant glioma: genetics and biology of a grave matter. *Genes Dev.* **15**, 1311–1333.
- McConkey D. J. and Orrenius S. (1996) Signal transduction pathways in apoptosis. *Stem Cells* **14**, 619–631.
- Mignotte B. and Vayssières J. L. (1998) Mitochondria and apoptosis. *Eur. J. Biochem.* **252**, 1–15.
- Mori A., Lehmann S., O'Kelly J., Kumagai T., Desmond J. C., Pervan M., McBride W. H., Kizaki M. and Koeffler H. P. (2006) Capsaicin, a component of red peppers, inhibits the growth of androgen-independent, p53 mutant prostate cancer cells. *Cancer Res.* **66**, 3222–3229.
- Petersen G., Moesgaard B., Schmid P. C., Schmid H. H. O., Broholm H. and Kosteljanetz M. (2005) Endocannabinoid metabolism in human glioblastomas and meningiomas compared to human non-tumor brain tissue. *J. Neurochem.* **93**, 299–309.
- Qiao S., Li W., Tsubouchi R., Haneda M., Murakami K. and Yoshino M. (2005) Involvement of peroxynitrite in capsaicin-induced apoptosis of C6 glioma cells. *Neurosci. Res.* **51**, 175–183.
- Santoni G., Perfumi M. C., Spreghini E., Romagnoli S. and Piccoli M. (1999) Neurokinin type-1 receptor antagonist inhibits enhancement of T cell functions by substance P in normal and neuromanipulated capsaicin-treated rats. *J. Neuroimmunol.* **93**, 15–25.
- Santoni G., Perfumi M. C., Pompei P., Spreghini E., Lucciarini R., Martarelli D., Staffolani M. and Piccoli M. (2000) Impairment of rat thymocyte differentiation and functions by neonatal capsaicin treatment is associated with induction of apoptosis. *J. Neuroimmunol.* **104**, 37–46.
- Santoni G., Amantini C., Lucciarini R., Perfumi M., Pompei P. and Piccoli M. (2004) Neonatal capsaicin treatment affects rat thymocyte proliferation and cell death by modulating substance P and neurokinin-1 receptor expression. *Neuroimmunomodulation* **11**, 160–172.
- Schwartzbaum J., Jonsson F., Ahlborn A., Preston-Martin S., Malmer B., Lonn S., Soderberg K. and Feychting M. (2005) Prior hospitalization for epilepsy, diabetes, and stroke and subsequent glioma and meningioma risk. *Cancer Epidemiol. Biomarkers Prev.* **14**, 643–650.
- Szallasi A. and Blumberg P. M. (1999) Vanilloid (capsaicin) receptors and mechanisms. *Pharmacol. Rev.* **51**, 159–211.
- Thompson C. B. (1995) Apoptosis in the pathogenesis and treatment of disease. *Science* **267**, 1456–1462.
- Wada T. and Penninger J. M. (2004) Mitogen-activated protein kinases in apoptosis regulation. *Oncogene* **23**, 2838–2849.
- Zhuang Z. Y., Xu H., Clapman D. E. and Ji R. R. (2004) Phosphatidylinositol 3-kinase activates ERK in primary sensory neurons and mediates inflammatory heat hyperalgesia through TRPV1 sensitization. *J. Neurosci.* **24**, 8300–8309.